

Analytical and Experimental Investigation of a Low Torque, Ultra-High Speed Drive System

C. Zwyssig, S.D. Round and J.W. Kolar
Power Electronic Systems Laboratory
ETH Zurich
8092 Zurich, Switzerland
zwyssig@lem.ee.ethz.ch

Abstract—New application areas are demanding the development of ultra-high speed electrical machines. Significant challenges exist to produce a test bench that is capable of withstanding operating speeds exceeding 500,000 rpm and measuring very low torque values of mNm. This paper describes a purpose built test bench that is able to characterize the operation of an ultra-high speed drive system. Furthermore, the calculation of electromagnetic losses, air friction and critical speeds is presented and a comparison of analytical and experimental results is given. The ultra-high speed machine has an efficiency of 95%, however, in the upper speed ranges the frictional losses become dominant.

I. INTRODUCTION

New application areas, such as generators/starters for micro gas turbines, turbo-compressor systems and drilling machines for medical tools and mechanical processing, are demanding the development of ultra-high speed electrical machines. Typically, the power ratings for these applications range from a few watts to a few kilowatts, and the speeds from a few tens of thousand rpm up to a million rpm [1]. The use of ultra-high speeds allows a very high power density to be achieved. New low loss magnetic materials and litz wire windings are required to counteract the high frequency losses and rare earth permanent magnets allow for a high torque density and elevated operating temperatures. Furthermore, advances in power electronic devices have allowed the development of small, efficient, high switching frequency inverters, while advances in digital signal processing technology has made the control of these ultra-high speed machines feasible.

For an ultra-micro gas turbine, a high-speed, permanent-magnet synchronous generator/starter has been developed [2]. It has a power output of 100 W for a rated speed of 500,000 rpm and a rated torque of 2 mNm. Initial tests have confirmed the results from the design stage. For this unique machine, different slotless winding structures and different stator core materials are to be compared in further testing to maximize the system efficiency. Furthermore, different topologies for the power electronics interface have been compared concerning size, weight, efficiency and control complexity [3].

In order to conduct accurate experimental verification of the machine design and critical speed calculation, and measure the efficiency of various machine and inverter configurations, an ultra-high-speed test bench has been built. Previously

reported high-speed test benches are realised using available hardware, such as mechanical couplings, ball bearings, torque transducers and temperature sensors, since the speed is limited to a few tens of thousand rpm, and the power is in the range of kW with a torque of Nm [4]. In contrast, significant challenges exist to produce a test bench that is capable of withstanding operating speeds exceeding 500,000 rpm, measuring very low torque values of mNm at high speeds and detecting critical speeds that cause very small vibrations.

This paper focuses on the ultra-high-speed test bench, measurement methods for torque, speed, power, losses, efficiency and critical speeds and the comparison of analytical and experimental data. First, a detailed description of the ultra-high-speed test bench is given, including the mechanical setup and the measuring equipment. Then, analytical analysis of the different losses is undertaken. Finally, experimental measurements are presented and compared to the analytical results.

II. TEST BENCH SETUP

As for normal size and speed machines, the test bench (Fig. 1)

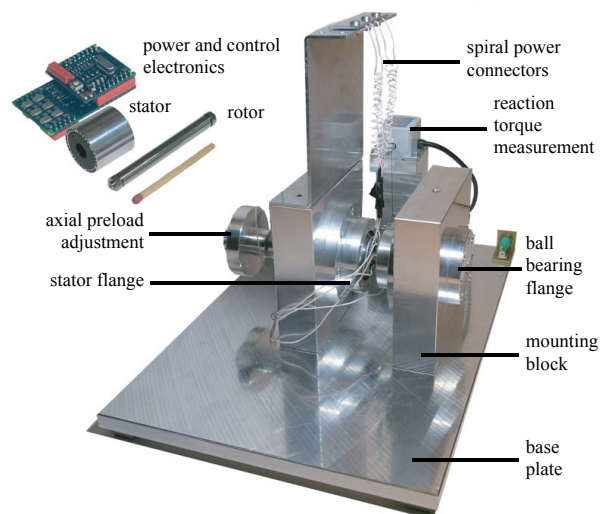


Figure 1. Ultra-high-speed test bench with motor in the right flange and generator in the left flange. The strain gauge force sensor in the back of the picture is attached to the moment arm with a thread to avoid shearing forces. The generator phases are connected via flexible spiral connections. On the left the single parts of the drive system (power and control electronics, stator, rotor) and their size compared to a match can be seen.

described here consists of two coupled machines with one operated as driving motor, and one as generator. All the different parts of the test bench are all mounted on a solid base plate, where two blocks hold the flanges for stators and bearings. Torque and speed measurement are required to determine the mechanical power and the losses. In this section, the mechanical construction is firstly presented, and then the measurement methods are described.

A. Rotor

At the rated speed of 500,000 rpm a mechanical coupling between motor and generator is not feasible. Therefore, the rotor is mechanically designed as common shaft for the two machines. The rotor consists of a titanium sleeve that includes two samarium-cobalt permanent magnets, one for each machine. The titanium sleeve, which also acts as shaft, is shrink-fitted onto the magnets in order to limit the stresses and guarantee torque transfer without gluing the magnets to the shaft. The rotor has a diameter of 6 mm and a total length of 55 mm.

B. Bearings

For machine speeds in the range of 500,000 rpm the selection of a suitable bearing is a main issue. Options for supporting a rotor are: aerostatic, aerodynamic or foil gas bearings, magnetic bearings or special high-speed ball bearings. Due to its simplicity and small size this test bench utilizes two radial single row high-speed ball bearings. One bearing is mounted on each end of the rotor and is held by an O-ring sitting in a flange. One of the flanges can be adjusted in axial direction in order to apply the required preload.

C. Stators

Two other flanges hold the two stators of motor and generator. The two identical stators consist of a three phase slotless litz wire winding, a laminated iron core and a cooling sleeve. For better heat conduction and electrical insulation the stators are sealed with an epoxy casting resin.

D. Power and control electronics

No commercial power electronic systems are available for drives up to speeds of 500,000 rpm since the fundamental frequency of the machine is 8.3 kHz. Therefore, custom built power and control electronics have been developed and realized in order to drive the machines [2]. The electronics are realized for low volume and weight and the control, including sensorless rotor position detection, is realized with a DSP.

E. Reaction torque measurement

The two stators each sit in flanges, where one is fixed to the frame of the test bench and the other is held radially and axially with ball bearings, but can rotate freely. With a moment arm connected to this stator the torque acting on it is transferred into a force, which can be measured with a force sensor.

This general setup has to be adapted for very low torques. The small force, for a moment arm h of 50 mm the rated torque of 1.9 mNm is translated into a force of 38 mN or a weight of 3.9 g, is measured with a special piezo-resistive force cell

(Huba Control Type 410) or an ultra-small-capacity strain gauge (Kyowa LVS-A). Furthermore, to suppress interference on the torque measurement, the ball bearings holding the stator are chosen for a minimal static friction and the influence of the connecting phase wires is minimized with a flexible connection realized with spiral wires (Fig. 1). However, achieving a good accuracy when measuring low torques is a difficult task and an area of research itself [5,6].

With this setup, the mechanical power on the shaft is not directly measured, but the reaction torque is measured on the stator of the machine. For generator operation this reaction torque includes the electromagnetic torque plus the parts of the air friction torque acting on the stator. The ball bearing friction reacts on the bearing block and is therefore not measured on the stator, and the measured power can be expressed as

$$\begin{aligned} P_{meas} &= P_{mech} - P_{f,bearing} \\ &= P_{el} + P_{Cu} + P_{core} + P_{f,air} \end{aligned} \quad (1)$$

with the power and losses according to Fig. 2.

F. Speed measurement and deceleration test

The rotational speed of the test bench can easily be extracted from a voltage or current waveform of a machine because the utilized machine is of synchronous type. In open-loop operation for example the rotational speed can be measured from the frequency of the back EMF, so no extra speed sensor is needed. Only at low speeds, where the amplitude of the induced voltage is very low, is the measurement difficult.

For measuring losses the deceleration test can be used. This method is based on the fact that in open loop operation (no electrical drive or break) the rotational energy is used up by the losses and the rotational speed decreases. The gradient of this deceleration is a measure for the losses. The dynamical equation for the rotor is

$$J \frac{d\omega}{dt} = -T_{Loss} = -\frac{P_{Loss}}{\omega} \quad (2)$$

where ω is the angular frequency and T_{Loss} is the total friction torque. The total losses P_{Loss} can be subdivided with two measurements when one of the losses is removed for the second measurement. The inertia J can be calculated with high accuracy due to the simple rotor geometry, the result is $J = 3.82 \cdot 10^{-8} \text{ kgm}^2$. Furthermore, the speed and its gradient have to be known. The speed measurement has to be smooth and exact in order to limit the error when differentiating.

II. ANALYTICAL CALCULATIONS

A. Loss analysis

In a high-speed machine, the losses can be split into iron losses in the stator core (P_{core}), copper losses in the winding (P_{Cu}), air friction losses due to windage ($P_{f,air}$) and ball bearing friction losses ($P_{f,bearing}$), as shown in Fig. 2. All of them can be determined analytically, except for ball bearing losses as at these high speeds no appropriate equations can be applied.

B. Stator core losses

In the machine configuration under investigation with a slotless winding and an ironless rotor, and therefore a large active air gap, the magnetic flux density in the stator core is produced by the permanent magnet and the influence from the stator winding is negligible. Therefore the iron losses in the stator core material can be calculated with a constant peak flux density B_m . For most soft magnetic materials the core losses can be calculated with the Steinmetz equation

$$P_{core} = C_m \cdot f^\alpha \cdot B_m^\beta \quad (3)$$

where C_m , α and β are taken from datasheets. In Fig. 3 it can be seen that for this machine the thinnest standard iron laminations (NOX20, silicon-iron, 168 μm laminations) have about 4.3 W losses at rated speed. Amorphous iron (Metglas iron based alloy 2605SA1) has about a tenth of these losses, and when designing the core for higher flux density (approximately 1 T) this ratio becomes even more extreme, therefore a future version of the machine will be built with an amorphous iron stator core.

In a machine the flux density is not distributed evenly in the stator core. In a cylindrical core as used in the machine here there is a flux concentration on the inner side in between the poles. For the calculation with the Steinmetz equation the mean value of the peak flux density over the radius of the stator core is used. Therefore it is important to verify this approximation with measurements. The total calculated core losses of the test bench, which includes two machines with NOX20 cores, can be seen in Fig. 7.

C. Stator winding losses

The copper losses in the winding of a machine are mainly due to dc resistance. For ultra-high speeds, the skin effect has also to be considered, and with a slotless winding the magnetic field penetrates through the copper and induces further eddy currents, which lead to additional losses. Therefore this machine has been built with a special litz-wire winding in order to reduce eddy-current losses. The calculation of the copper losses and the optimization of the litz-wire winding has been presented in [2]. As described in the previous section the magnetic field is practically independent of the stator current, and therefore are eddy-current losses due to the external magnetic field (usually called proximity effect losses) only dependent on speed. With utilizing a litz-wire winding the skin effect becomes negligible. With the electrical torque being proportional to the phase currents the total copper losses can be calculated against speed and torque. For sinusoidal alternating currents and magnetic fields the losses are calculated and plotted in Fig. 4.

D. Air friction losses

For ultra-high speed machines air friction losses become significant, especially because they scale with the third power of the rotational speed. Therefore, the friction losses of a long rotating cylinder encased in another cylinder are calculated. The air friction losses on the end caps are neglected. The

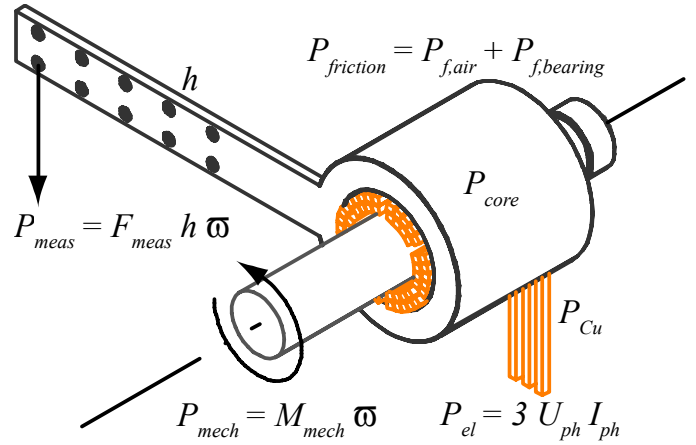


Figure 1. Localization of the different losses for a high speed machine. P_{meas} and P_{el} can be measured. P_{mech} is the input power and P_{el} the output power for generator operation, or vice versa for motor operation.

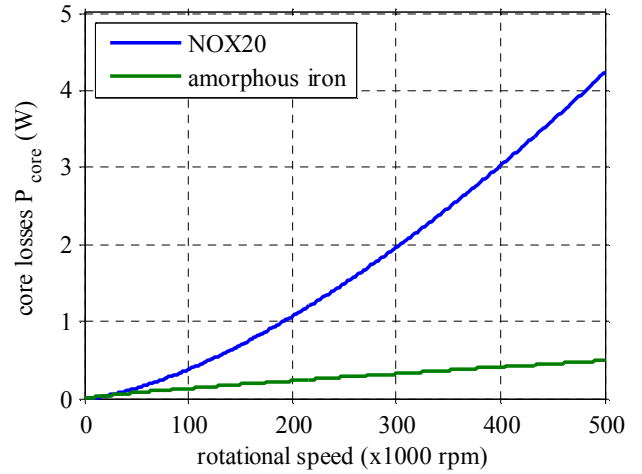


Figure 2. Calculated stator core losses in the high-speed machine. The core volume V is 1.6 cm^3 and the peak induction B_m is 0.5 Tesla.

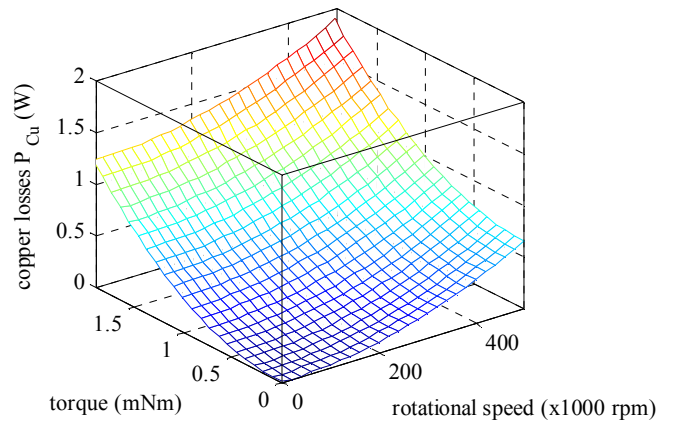


Figure 3. Total copper losses of one machine versus rotational speed and electrical torque.

general equation for air friction losses is

$$P_{f,air} = c_f \pi \rho_{air} \omega^3 r^4 l \quad (4)$$

where ρ_{air} is the density of the surrounding air, ω is the angular frequency, r is the radius and l the length of the cylinder. The friction coefficient c_f is dependent on the radius of the cylinder, the air gap s to the housing (stator), the Reynolds (Re) and the Taylor (Ta) number, which are defined as

$$Re = \frac{r^2 \omega}{\nu}, Ta = \frac{r \omega s}{\nu} \sqrt{\frac{s}{r}} \quad (5)$$

where ν is the viscosity of air. It can be seen that these numbers are again dependent on speed again. The flow stability depends on the Taylor number, and it can be divided into a laminar Couette flow ($Ta < 41.3$), laminar flow with Taylor vortices ($41.3 < Ta < 400$) and turbulent flow ($Ta > 400$).

For laminar Couette flow the friction coefficient can be determined analytically, but measurements show discrepancies with the theoretical values, therefore empirical data is usually used and correction factors are applied to adapt for different geometries. For the air gap of the machine under investigation the friction coefficient has been determined in [7] as

$$c_f = \frac{1.8}{Re} \left(\frac{s}{r}\right)^{-0.25} \frac{(r+s)^2}{(r+s)^2 - r^2} \quad (6)$$

In the turbulent flow area measurements show a friction coefficient that is proportional to

$$c_f \propto Ta^{-0.2} \quad (7)$$

Fig. 5 shows the values of the friction coefficients versus Reynolds number used for estimating the friction losses with (4). Fig. 6 shows the calculated friction losses versus speed for one machine. It can be seen that above a speed of 88,000 rpm the air flow in the air gap is fully turbulent. At rated speed the air friction losses already reach 7.8 W and are therefore a main contributor to the total losses at high speeds. Because air friction coefficients are based on empirical data the air friction losses are verified experimentally.

E. Total test bench losses

The test bench incorporates two machines, therefore all the losses have to be doubled for comparison with the measurements. Fig. 7 shows the individual contribution and the summation of the losses versus speed. The copper losses are calculated for open loop (no electrical torque) operation. The ball bearing losses are not shown as they can not be determined analytically. Therefore the friction losses in the bearings have to be determined experimentally.

F. Efficiency

Beside the knowledge of the individual loss contributions a goal of the loss analysis is the determination of the efficiency, η , of the entire machine. A drawing of the machine, its losses, input and output power and the measurement setup is shown in Fig. 2. Generally, the efficiency is defined as

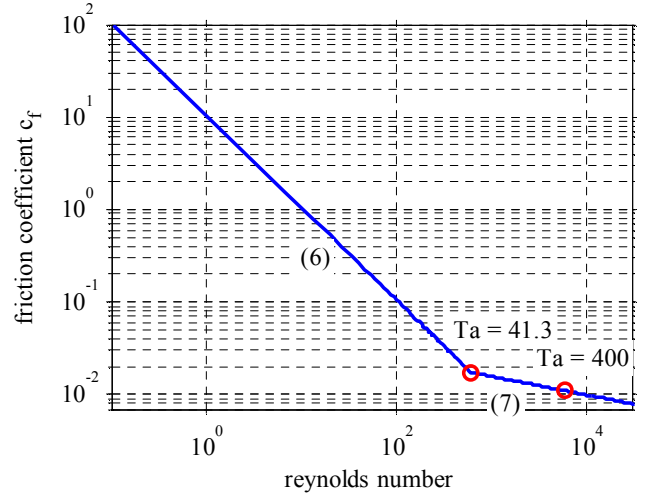


Figure 4. Friction coefficient versus Reynolds number for calculating the friction losses of one ultra-high speed machine.

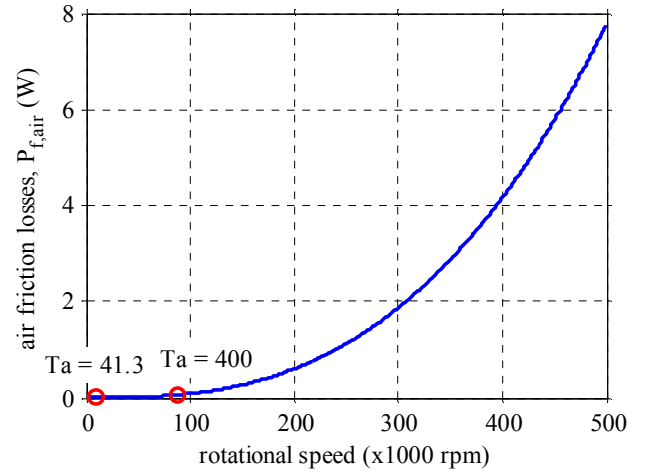


Figure 5. Air friction losses versus speed of one ultra-high speed machine. Above 88,000 rpm the air flow in the air gap is turbulent.

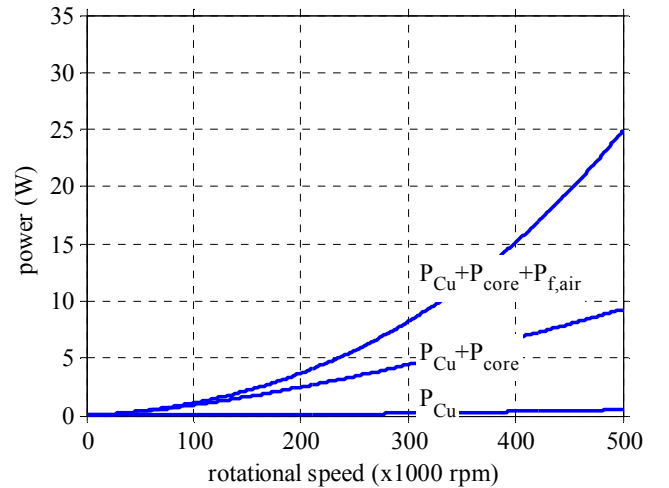


Figure 6. Calculated losses of the test bench (two machines) for open loop (no electrical torque) operation. Ball bearing losses and therefore total losses can not be calculated.

$$\eta = \frac{P_{out}}{P_{in}} = \frac{P_{in} - P_{Loss}}{P_{in}} \quad (8)$$

where for generator operation P_{in} is the mechanical power P_{mech} and for motor operation the electrical power P_{el} . The power losses P_{Loss} consist of the individual losses.

A high-speed system with speeds in the area of 500,000 rpm will always be an integrated mechanical design. Therefore it is difficult to allot friction losses to either the electrical machine or the rest of the system. For example, turbine manufacturers consider bearing losses as part of the turbomachinery [8] and in an air spindle all windage losses are part of the air bearing system. In contrary to that, in a turbocompressor system the resulting mechanical power delivered to the compressor wheel is important and the friction torque is deducted from the electrical torque. Therefore, no universal definition of the efficiency of an ultra-high speed electrical machine can be given, as it is always dependent on the application. Only considering electromagnetic losses ($P_{Loss} = P_{Cu} + P_{core}$) the calculated efficiency of one machine at rated speed and power then is 96%. If also air friction losses are considered ($P_{Loss} = P_{Cu} + P_{core} + P_{f,air}$), the efficiency drops down to 86%, and the bearing losses are not yet considered.

III. EXPERIMENTAL INVESTIGATION

A. Reaction torque measurement

One important measurement for verifying the data obtained at the design stage is the torque per phase current ratio. This is obtained by driving the motor of the test bench and connecting a variable resistive load to the generator side. The reaction torque on the generator stator can be measured with the setup described in section II.E. In Fig. 8 it is shown that the predicted and measured torque values match very well.

B. Back EMF measurement

The second important measurement for verifying the data obtained at the design stage is the back EMF measurement. This can be performed by driving the motor of the test bench at rated speed and measuring the open-loop phase voltage on the generator side. The 16 V peak measured at 500,000 rpm exactly matches the value given by the design calculations (Fig. 9).

C. Efficiency measurements via reaction torque

When operating as a generator, the efficiency incorporating copper, core and air friction losses can be measured by comparing the mechanical power measured $P_{in} = P_{meas}$ and the electrical output power $P_{out} = P_{el}$ measured with a three phase power analyzer, according to Fig. 2 and (1,8).

For low speeds the output power is very low due to the low voltage and therefore the losses outweigh the output power and this results in a low efficiency. At high speeds the efficiency decreases, which is mainly due to the increase in air friction losses and to a lesser extent due to an increase in core losses and copper eddy current losses. Fig. 10 shows the comparison of the measured and the calculated efficiency for a torque of

1 mNm and up to half of the rated speed. At higher speeds the scattering of the measurements gets bigger due to vibrations.

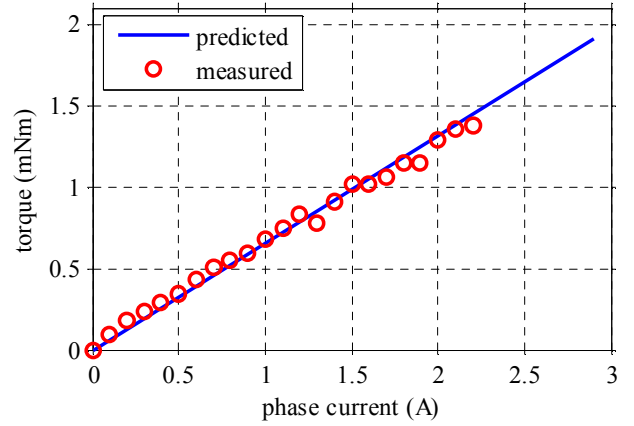


Figure 7. Comparison of predicted and measured torque over phase current.

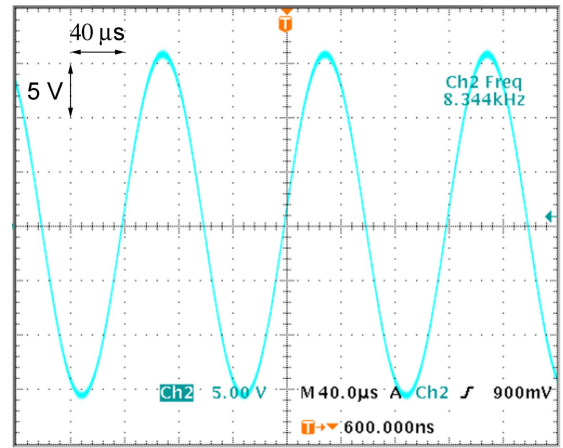


Figure 8. Open-loop phase voltage (back EMF) at 500,000 rpm.

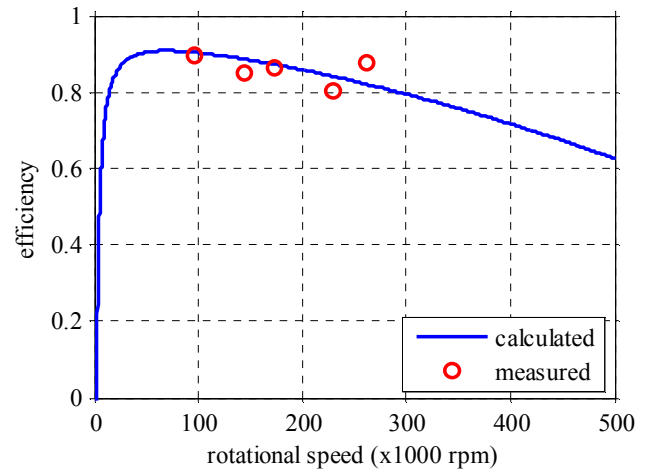


Figure 9. Comparison of calculated and measured efficiency for an electrical torque of 1 mNm (half the rated torque). Copper losses, core losses and air friction losses are included in measurement and calculation according to (3).

The variations in the measurements are mainly due to the sensitive torque measurement, the friction in the ball bearings holding the generator stator, the influence by the cabling and vibrations of the test bench. For a more exact measurement of the efficiency and the different losses all these problems would have to be tackled, but measurements with the deceleration test are more exact.

D. Loss measurements via deceleration test

For these measurements the test bench is spun up to approximately 600,000 rpm and then the drive system is switched off such that just the losses decelerate the rotor. The speed is measured over time from the back EMF with a LabView interface and the speed gradient, friction torque and loss power are calculated in matlab.

With the normal deceleration test the total losses in open-loop operation are determined, which include copper, core, air friction and bearing friction losses. The total losses at 500,000 rpm and no electrical torque are 35 W for the entire test bench, which consists of two machines and two ball bearings. The whole losses over speed are shown in Fig. 11. The power over rotational speed curve could also be influenced by power needed for vibrations, for example when passing critical speeds or when oscillations of other parts of the test bench are excited. For example every measurement shows a steeper gradient in the area of 450,000 rpm.

For a second measurement the test bench is placed in vacuum in order to have negligible air friction losses. Two measurements from a start speed of 400,000 rpm were successful, but the ball bearings failed at rated speed. The reasons for the failure are that no cooling exists because of the absence of cooling air and the vaporization of the lubricant. Nevertheless the measurements show a difference, and the air friction losses can be experimentally determined. The experimental results match the calculations very well as can be seen in Fig. 11. From knowing the total and the individual losses except bearing friction losses those must be the difference.

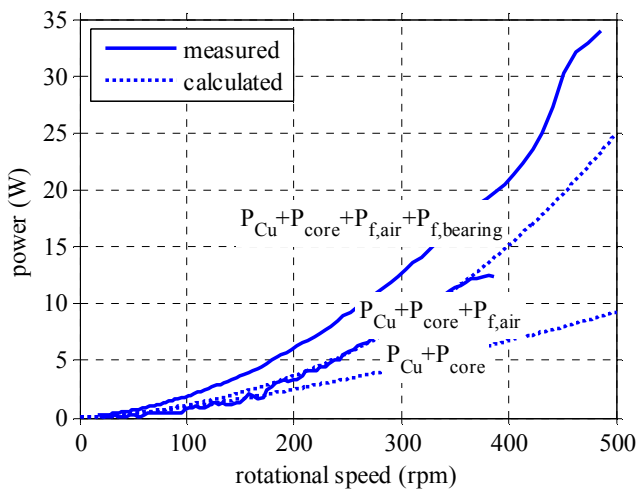


Figure 10. Measured losses of the test bench over speeds. The total power losses are subdivided into bearing losses, windage losses and core losses.

All the losses except ball bearing losses have to be halved in order to have the individual losses for one machine, because of the two machines assembled on the test bench. In Table I the individual losses for one machine at rated speed (500,000 rpm) and rated torque (1.9 mNm) are shown. The copper losses are taken from Fig. 4, the core losses are calculated with (3), the air friction are calculated with (4) and verified by experiments shown in Fig. 11, where also the ball bearing losses are extracted from.

E. Critical speed measurements

In order to verify the critical speeds obtained by calculations vibration measurements have to be undertaken. Measurements with an accelerometer show no significant results since the vibrations are too small. Therefore, measurements are carried out using a polytec laser vibrometer directed onto a not rotating part of the test bench, for example the flanges of the ball bearings.

The critical speeds have been calculated analytically and with finite element simulations for the rotor of the test bench in [2]. The bearing stiffness is included in the calculations, but the O-rings holding the bearings can shift the critical speeds and no method exists to estimate or even calculate the influence of O-rings. Nevertheless, Table II shows a good agreement of predicted and measured critical speeds for the titanium rotor.

IV. CONCLUSION

Emerging application areas such as micro gas turbines, drilling spindles and compressor systems are demanding the development of ultra-high-speed electrical drive systems. A 500,000 rpm, 100 W electrical machine and suitable power and control electronics have previously been designed and constructed. For the experimental investigation of such an electrical drive system, significant challenges exist to produce a test bench that is capable of withstanding operating speeds exceeding 500,000 rpm and measuring very low torque values of mNm at high speeds.

This paper has presented a suitable test bench design and measurement methods that are able to characterize the operation of an ultra-high-speed machine. The test bench is constructed by using a one piece rotor for the motor and

TABLE I. LOSSES FOR ONE MACHINE AT RATED SPEED AND TORQUE

Copper losses	1.9 W
Core losses	4.3 W
Air friction losses	8 W
Ball bearing losses, two bearings	10 W

TABLE II. CRITICAL SPEEDS

	Calculation	Measurement
First critical speed	2400 Hz	2400 Hz
Second bending mode	4250 Hz	4400 Hz
Third bending mode	9880 Hz	not measured

generator machines, high-speed ball bearings, and a stator mounted torque measurement system. The very low reaction torque values are difficult to measure, but match the calculated values obtained at the design stage. For more exact measurements the deceleration test is the preferred measurement method.

For the loss analysis of this small ultra-high-speed machine the losses are subdivided into copper losses, core losses, air and ball bearing friction losses. All except ball bearing losses are calculated independently and the comparison with experimental measurements performed using the test bench show a good agreement. The ball bearing losses are determined experimentally.

The efficiency of the machine is very much dependent on the allocation of the losses to either the electrical drive system or the application. With defining the friction losses as part of the application (for example in a gas turbine or an air bearing drilling spindle) the efficiency of the machine is 95% at rated speed and power. Allocating the losses to the drive system (for example for a turbocompressor system) the efficiency drops down to 75%. With the electromagnetic design already optimized for high speed operation, the friction losses become dominant and for an improvement in total system efficiency of an ultra-high speed low power drive system the focus has to be on minimizing the bearing and air friction losses.

REFERENCES

- [1] M.A. Rahman, A. Chiba, and T. Fukao, "Super high speed electrical machines – summary," IEEE Power Engineering Society General Meeting, June 6-10, 2004, vol. 2, pp. 1272-1275.
- [2] C. Zwyszig, J.W. Kolar, W. Thaler, M. Vohrer, "Design of a 100 W, 500000 rpm permanent-magnet generator for mesoscale gas turbines," IEEE Industry Applications Conference 2005, Conference Record of the 40th IAS Annual Meeting, Hong Kong, October 2-6, 2005, vol. 1, pp. 253-260.
- [3] C. Zwyszig, S.D. Round and J.W. Kolar, "Power Electronics Interface for a 100 W, 500000 rpm Gas Turbine Portable Power Unit," Applied Power Electronics Conference, Dallas, Texas, USA, March 19-23, 2006, pp. 283-289.
- [4] O. Aglen, "Back-to-back tests of a high-speed generator," IEEE International IEEE Electric Machines and Drives Conference, June 1-4, 2003, vol. 2, pp. 1084-1090.
- [5] H. Ota1, T. Ohara, Y. Karata, S. Nakasima and M. Takeda1, "Novel micro torque measurement method for microdevices," Journal of Micromechanics and Microengineering, vol. 11, no. 5, 2001, pp. 595-602.
- [6] V. Gass, B.H. van der Schoot, S. Jeanneret, N.F. de Rooij, "Micro-torque sensor based on differential force measurement," IEEE Workshop on Micro Electro Mechanical Systems, 1994, Oiso, January 25-28, 1994, pp. 241-244.
- [7] M. Mack, "Luftreibungsverluste bei elektrischen Maschinen kleiner Baugröße," Ph.D. dissertation, Universität Stuttgart, Germany, 1967.
- [8] O. Aglén, "Loss calculation and thermal analysis of a high-speed generator," IEEE International Electric Machines and Drives Conference IEMDC, Madison, Wisconsin, USA, June 2003.